

Effects of Drug Resistance Mutations L100I and V106A on the Binding of Pyrrolobenzoxazepinone Nonnucleoside Inhibitors to the Human Immunodeficiency Virus Type 1 Reverse Transcriptase Catalytic Complex

Giada A. Locatelli,¹ Giuseppe Campiani,² Reynel Cancio,¹ Elena Morelli,² Anna Ramunno,² Sandra Gemma,² Ulrich Hübscher,³ Silvio Spadari,¹ and Giovanni Maga^{1*}

Istituto di Genetica Molecolare IGM-CNR, Consiglio Nazionale delle Ricerche, 27100 Pavia,¹ and Dipartimento Farmaco Chimico Tecnologico and European Research Center for Drug Discovery and Development, Siena University, 53100 Siena,² Italy, and Institute of Veterinary Biochemistry and Molecular Biology, University of Zürich-Irchel, CH-8057 Zurich, Switzerland³

Received 11 November 2003/Returned for modification 8 January 2004/Accepted 21 January 2004

We have previously described a novel class of nonnucleoside reverse transcriptase (RT) inhibitors, the pyrrolobenzoxazepinone (PBO) and the pyridopyrrolooxazepinone (PPO) derivatives, which were effective inhibitors of human immunodeficiency virus type 1 (HIV-1) RT, either wild type or carrying known drug resistance mutations (G. Campiani et al., *J. Med. Chem.* 42:4462–4470, 1999). The lead compound of the PPO class, (R)-(-)-PPO464, was shown to selectively target the ternary complex formed by the viral RT with its substrates nucleic acid and nucleotide (G. Maga et al., *J. Biol. Chem.* 276:44653–44662, 2001). In order to better understand the structural basis for this selectivity, we exploited some PBO analogs characterized by various substituents at C-3 and by different inhibition potencies and drug resistance profiles, and we studied their interaction with HIV-1 RT wild type or carrying the drug resistance mutations L100I and V106A. Our kinetic and thermodynamic analyses showed that the formation of the complex between the enzyme and the nucleotide increased the inhibition potency of the compound PBO354 and shifted the free energy (energy of activation, ΔG^\ddagger) for inhibitor binding toward more negative values. The V106A mutation conferred resistance to PBO 354 by increasing its dissociation rate from the enzyme, whereas the L100I mutation mainly decreased the association rate. This latter mutation also caused a severe reduction in the catalytic efficiency of the RT. These results provide a correlation between the efficiency of nucleotide utilization by RT and its resistance to PBO inhibition.

The virus-encoded human immunodeficiency virus type 1 (HIV-1) reverse transcriptase (RT) is a major target for antiviral chemotherapy (18, 20). Two classes of inhibitors are targeted to the viral RT: nucleoside RT inhibitors (NRTIs) and nonnucleoside RT inhibitors (NNRTIs) (9, 11, 28). The latter compounds are highly specific for HIV-1 RT and bind to the enzyme at an allosteric site close distinct from the catalytic site, behaving as typical noncompetitive inhibitors with respect to the different substrates of the polymerization reaction (12, 23). The NNRTIs nevirapine, delavirdine, and the most recently licensed, efavirenz, are currently used in clinical practice (8) and are characterized by less-severe adverse effects than NRTIs or protease inhibitors (PIs) (26). Combinations of NNRTIs with NRTIs and PIs, have been shown to suppress plasma HIV-1 load longer than monotherapy or dual therapy, allowing CD4T cell increase, immune system function restoration, and clinical improvement (22, 35). However, the occurrence of just a few single amino acid substitutions in the RT gene can confer resistance to most of the NNRTIs (14, 26, 29). Therefore, the development of novel NNRTIs with improved

pharmacological, pharmacokinetic, and drug resistance mutation profiles is critical for a more successful application of NNRTIs in combination therapy. We have previously described a novel class of NNRTIs based on an oxazepinone skeleton, namely, pyrrolobenzoxazepinone (PBO) and pyridopyrrolooxazepinone (PPO) derivatives, which were effective inhibitors of HIV-1 RT, either wild type or carrying known drug resistance mutations. Compared to the reference compound nevirapine, several of the synthesized PBOs and PPOs displayed a higher inhibitory activity against wild-type RT and clinically relevant mutant RTs containing the single amino acid substitutions L100I, K103N, V106A, Y181I, and Y188L (7). In addition, we have shown that the lead compound of this class, (R)-(-)-PPO464, was selectively targeting the ternary complex formed by the viral RT with its substrates nucleic acid and nucleotide. It showed a significant synergy with the NRTI zidovudine and a favorable pharmacokinetic profile in mice and rats, either alone or during coadministration with the HIV-1 PI ritonavir (25). The results of the biological and pharmacokinetic experiments suggest a potential clinical utility of PBO and PPO analogs in combination with NRTIs against strains of HIV-1 bearing mutations that confer resistance to known NNRTIs. Due to the potential interest of PBOs as novel NNRTIs, we sought to further investigate their mechanism of action. For this purpose, we selected some PBO ana-

* Corresponding author. Mailing address: Istituto di Genetica Molecolare IGM-CNR, Consiglio Nazionale delle Ricerche, via Abbiategrasso 205, 27100 Pavia, Italy. Phone: 39-0382-546355. Fax: 39-0382-422286. E-mail: maga@igm.cnr.it.

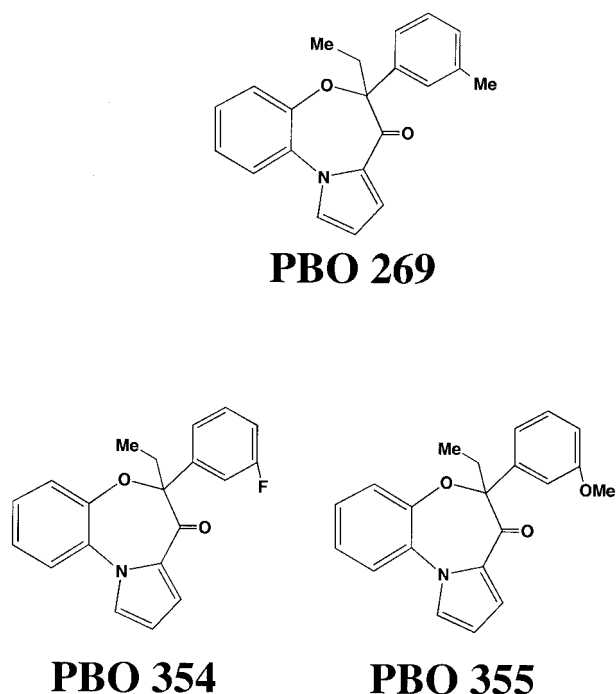


FIG. 1. Structures of the PBO analogs used in the present study.

logs (Fig. 1) with different inhibition potencies and drug resistance profiles. In particular, we selected PBO354 because, uniquely among the PBO derivatives originally developed, showed significant reduced activity toward HIV-1 RT carrying the L100 I and V106A mutations, and we compared it to the closely related compounds NF269 and NF355, which, on the other hand, had similar potencies against both mutants with respect to the wild-type RT (7). Remarkably, PBO354 proved also to be among the less-toxic compounds of the PBO class on a variety of cell lines (7). We then studied the interaction of these compounds with HIV-1 RT wild type or carrying the drug resistance mutations L100I and V106A.

MATERIALS AND METHODS

Inhibitors. The PBO derivatives shown in Fig. 1 were synthesized as previously described (7). Azidothymidine triphosphate (AZTTP) was obtained from Amersham Biosciences.

Nucleic acid substrates. The homopolymers poly(rA) or poly(dA) (Amersham Biosciences) were mixed at weight ratios in nucleotides of 10:1 to the oligomer oligo(dT)₁₂₋₁₈ (Amersham Biosciences) in 20 mM Tris-HCl (pH 8.0) containing 20 mM KCl and 1 mM EDTA, heated at 65°C for 5 min, and then slowly cooled at room temperature. Calf thymus-activated DNA was prepared as described previously (37).

Expression and purification of recombinant HIV-1 RT forms. The coexpression vectors pUC12N/p66(His)/p51 with the wild-type HIV-1 RT p66/p51 or the point mutants L100I/p66/p51 and V106A/p66/p51 (6) were kindly provided by S. H. Hughes (NCI-Frederick Cancer Research and Development Center) and purified in two steps as described previously (24). Recombinant RT was purified to >95% purity and had poly(rA)/oligo(dT) specific activities (see below) of 75,670 U/mg for RT wild type, 56,690 U/mg for RT L100I, and 62,760 U/mg for RT V106A; 1 U of DNA polymerase activity corresponds to the incorporation of 1 nmol of deoxynucleotide monophosphate (dNMP) into acid-precipitable material in 60 min at 37°C. The identity of the introduced mutations was confirmed by sequencing (6).

HIV-1 DNA polymerase activity assay. RNA- or DNA-dependent DNA polymerase activity was assayed as follows: a final volume of 25 μ l contained buffer A (50 mM Tris-HCl [pH 7.5], 1 mM dithiothreitol, 0.2 mg of bovine serum

albumin/ml, 4% glycerol), 10 mM MgCl₂, 0.5 μ g of either poly(rA)/oligo(dT)_{1:10} or poly(dA)/oligo(dT)_{1:10} (0.3 μ M 3'-OH ends), [³H]dTTP (1 Ci/mmol) as indicated in the figure legends, and 2 to 4 nM RT. Reactions were incubated at 37°C for the indicated times. When activated DNA was used, [³H]deoxynucleoside triphosphates (dNTPs; 4 Ci/mmol) were added in place of dTTP, in the presence of 0.04 mg of the DNA template/ml. Then, 20 μ l-aliquots were spotted onto glass fiber filters (GF/C), which were immediately immersed in 5% ice-cold trichloroacetic acid. Filters were washed twice in 5% ice-cold trichloroacetic acid and once in ethanol for 5 min and then dried, and acid-precipitable radioactivity was quantitated by scintillation counting.

Inhibition assays. Reactions were performed under the conditions described for the HIV-1 RT RNA- or DNA-dependent DNA polymerase activity assay. Incorporation of radioactive dTTP into poly(rA)/oligo(dT) or poly(dA)/oligo(dT) at different concentrations of dTTP was monitored in the presence of increasing amounts of inhibitor as indicated in the figure legends.

Kinetics of inhibitor binding. HIV-1 RT (20 to 40 nM) was incubated 2 min at 37°C in a final volume of 4 μ l in the presence of buffer A, 10 mM MgCl₂, 100 nM 3'-OH ends, and 10 μ M unlabeled dTTP (for the formation of the RT/TP/dNTP complex). The inhibitor to be tested was then added to a final volume of 5 μ l at a concentration at which the $[E]/[E_0]$ was $(1 - 1/[1 + [I]/K_i]) > 0.9$. Then, 145 μ l of a mix containing buffer A, 10 mM MgCl₂, and 10 μ M [³H]dTTP (5 Ci/mmol) were added at different time points. After an additional 10 min of incubation at 37°C, 50- μ l aliquots were spotted on GF/C filters, and the acid-precipitable radioactivity was measured as described for the HIV-1 RT RNA-dependent DNA polymerase activity assay. The quantity (v_t/v_0) representing the normalized difference between the amounts of dTTP incorporated at the zero time point and at the different time points was then plotted against time.

Kinetic parameter calculation. All values were calculated by non-least-squares computer fitting of the experimental data to the appropriate rate equations. K_m and k_{cat} values were calculated according to the Michaelis-Menten equation by analyzing the variation of the initial velocities of the reaction in dependence on the substrate concentration. Time-dependent incorporation of radioactive dTTP into poly(rA)/oligo(dT) at different substrate concentrations was monitored by removing 20- μ l aliquots at the 2-, 4-, 6-, and 12-min time points. The initial velocities of the reaction, determined by linear regression analysis of the data, were then plotted against the corresponding substrate concentrations.

K_{app} values for the ternary complex were calculated according to the equation for noncompetitive inhibition:

$$v = V_m / [(K_m/[S]) + (1 + [I]/K_{app})] \quad (1)$$

The true equilibrium dissociation constant (K_i) was calculated from the variation of K_{app} as a function of the dTTP concentrations according to the equation:

$$K_{app} = [1 + (K_m/[S])]K_i \quad (2)$$

The apparent binding rate (k_{app}) values were determined by fitting the experimental data to the single-exponential equation:

$$(v_t/v_0) = e^{-k_{app}t} \quad (3)$$

where t is time. If $[E]_0$ is the input enzyme concentration, $[E]$ is the enzyme available for the reaction at time t , and $[E]_i$ is the enzyme bound to the inhibitor at time t , it follows that $[E]_t = [E]_0 - [E]_i$. Since $v_0 = k_{cat}[E]_0$ and $v_t = k_{cat}[E]_t$, then $v_t/v_0 = 1 - [E]_i/[E]_0$. Thus, the v_t/v_0 value is proportional to the fraction of enzyme bound to the inhibitor.

The true association (k_{on}) and dissociation (k_{off}) rates were calculated from the relationships:

$$k_{on} = k_{app}/([I] + K_i) \text{ and } k_{off} = k_{on}K_i$$

For the thermodynamic parameters calculations, ΔH^\ddagger and ΔS^\ddagger values for inhibitor binding were determined according to the van't Hoff equation:

$$\ln(1/K_{app}) = -\Delta H^\ddagger/RT + \Delta S^\ddagger/R \quad (4)$$

where R is the gas constant and T the absolute temperature (in Kelvins).

ΔG^\ddagger (energy of activation) was calculated from the equation:

$$\Delta G^\ddagger = \Delta H^\ddagger - T\Delta S^\ddagger$$

The variation of ΔG^\ddagger as a function of the dTTP concentration was analyzed according to the equation:

$$\Delta G^\ddagger = RT \ln[(1 + K_m/[S])K_i] \quad (5)$$

The thermodynamic parameters for dTTP incorporation were calculated according to the Eyring equation:

$$\ln(k_{\text{cat}}/T) = -\Delta H/T + \ln(k_b/h) + \Delta S/R \quad (6)$$

where k_b is Boltzmann's constant, h is Planck's constant, R is the gas constant, and T is the absolute temperature (Kelvin).

The buffering system used (Tris-HCl [pH 7.]) is sensitive to the temperature. However, in the range of temperatures used for the reactions, the variation was comprised from pH 7.6 to 7.2, which corresponds to the 90% activity pH range of HIV-1 RT.

RESULTS

Inhibition of HIV-1 RT by the PBO class of inhibitors dependent on substrate binding by the enzyme. We have previously shown that the NNRTI (*R*)-(-)-PPO464 specifically targets the catalytically competent ternary complex of RT with its nucleic acid and nucleotide substrates (25). As a consequence, the potency of inhibition of (*R*)-(-)-PPO464 was shown to increase as the concentration of the substrates was increased. In order to verify whether this property was common to the PBO class of antiviral agents, wild-type HIV-1 RT was challenged with the inhibitors PBO269, PBO354, and PBO355 (shown in Fig. 1). According to the ordered mechanism of the polymerization reaction, whereby template-primer (TP) binds first, followed by the addition of dNTP, the HIV-1 RT can be present in three different catalytic forms: as a free enzyme, in a binary complex with the TP and in a ternary complex with T/P and dNTP (21). Thus, when the TP substrate was held constant at a saturating concentration and the dependence of the inhibition for various concentrations of dNTPs was analyzed at the steady state, all of the input RT was in the form of the RT-TP binary complex, and only two forms of the enzyme (the binary complex and the ternary complex with dNTP) could react with the inhibitor. Similarly, when the dNTP concentration was kept constant at saturating levels and the dependence of the inhibition was analyzed at various TP concentrations, RT was present either as a free enzyme or in the ternary complex with TP and dNTP. Thus, in both cases simple steady-state kinetic analysis could be used for the determination of the equilibrium dissociation constants of the different enzyme-inhibitor complexes. When wild-type HIV-1 RT was challenged with the compound PBO354 in the presence of a saturating amount of RNA/DNA substrate poly(rA)/oligo(dT) and in the presence of increasing concentrations of the nucleotide substrate TTP the observed inhibition was of the noncompetitive type (Fig. 2A). Similar results were obtained when wild-type RT was challenged with different concentrations of PBO354 in the presence of increasing concentration of the nucleic acid substrate [RNA/DNA substrate poly(rA)/oligo(dT)] and saturating amounts of the nucleotide dTTP (Fig. 2B). By using this approach, the apparent inhibition constants (K_{app}) for all of the different inhibitors were then determined, and their variation in dependence of the nucleotide substrate concentrations is shown in Fig. 2C. All of the inhibitors tested showed an increase in potency (reduction of K_{app} values), which was dependent on the TTP concentrations. From these data it was possible to calculate the true inhibition constant (K_i) for each inhibitor. The derived values are listed in Table 1. The compound PBO354, bearing a fluorine atom at position 3 of the pendant phenyl ring, showed the

TABLE 1. Kinetic and thermodynamic parameters for binding of PBO derivatives to HIV-1 RT

| Parameter | Mean value (SD) ^a | | | | | | | | | | | |
|--|------------------------------|------------|--------------|--------------------------|--------|-------------|------------|------------------------|---------|-------------|-------------|----------------------------|
| | Wild type | | | | | | V106A | | | | | |
| | NVP | PBO269 | PBO355 | PBO354 | NVP | PBO269 | PBO355 | PBO354 | NVP | PBO269 | PBO355 | PBO354 |
| K_i (μM) | 0.4 (0.06) | 0.1 (0.02) | 0.085 (0.01) | 0.03 (0.002) | 10 (1) | 0.25 (0.03) | 0.1 (0.01) | 0.08 (0.01) | 9 (0.7) | 0.17 (0.02) | 0.12 (0.01) | 0.7 (0.1) |
| k_{on} ($\text{s}^{-1} \mu\text{M}^{-1}$) | | | | 0.01 (0.002) | | | | 0.01 (0.002) | | | | 0.002 (-0.0001) |
| k_{off} (s^{-1}) | | | | $3 (0.4) \times 10^{-4}$ | | | | $8 (1) \times 10^{-4}$ | | | | $1.4 (0.2) \times 10^{-3}$ |
| ΔH^\ddagger (kcal mol ⁻¹) | | | | 6 (0.5) | | | | 10 (1) | | | | 12 (1) |
| ΔS^\ddagger (cal mol ⁻¹ K ⁻¹) | | | | 22 (3) | | | | 34 (5) | | | | 39 (4) |
| $\Delta G^\ddagger_{(310)^\text{b}}$ (kcal mol ⁻¹) | | | | -0.82 (0.1) | | | | -0.54 (0.02) | | | | -0.09 (-0.004) |

^a NVP, nevirapine. Values for the kinetic parameters represent the mean of three independent experiments.

^b $\Delta G^\ddagger_{(310)}$, energy of activation at 310 K.

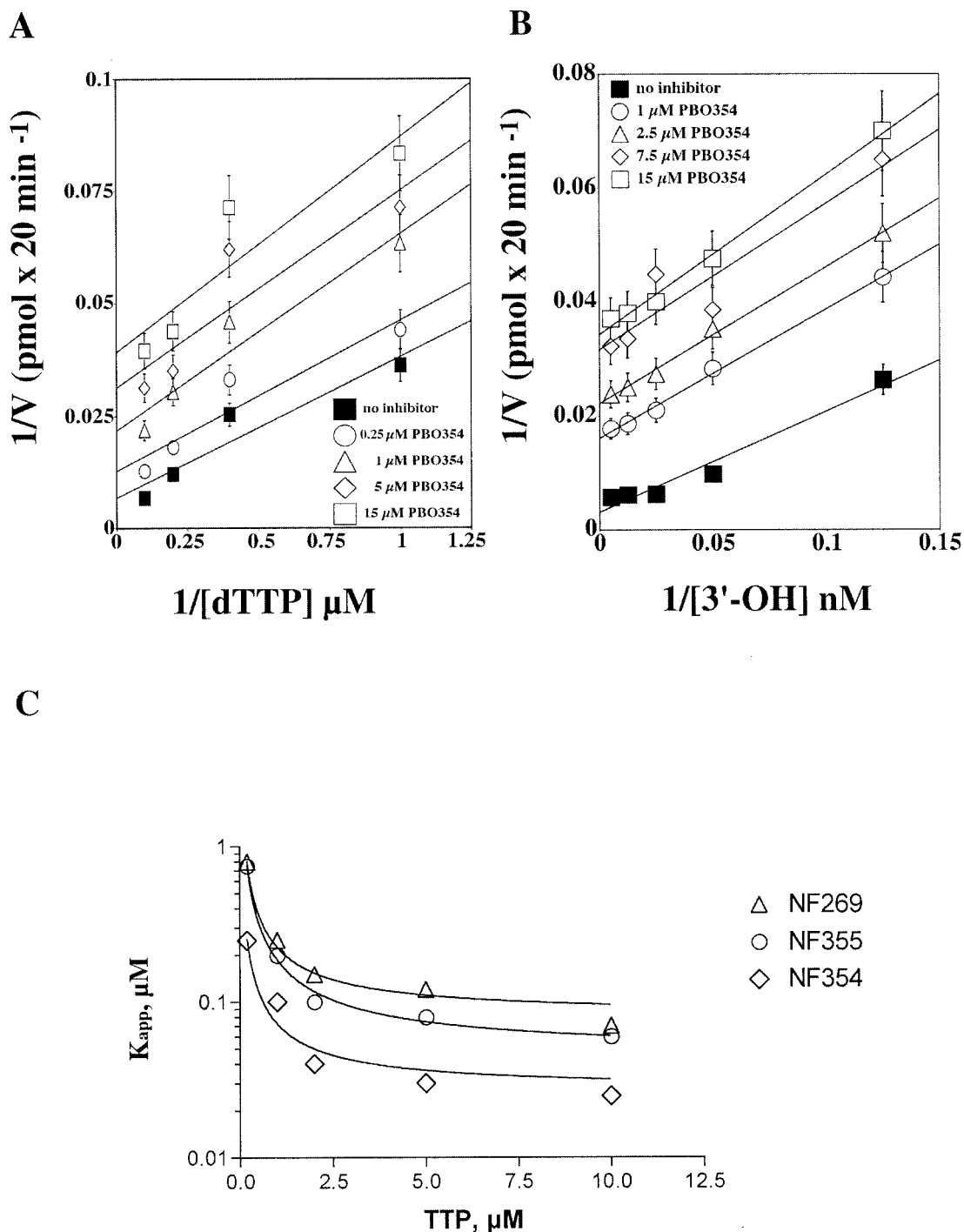


FIG. 2. All of the datum points represent the mean values of three independent experiments. Error bars indicate the standard deviations. (A) HIV-1 RT wild type was tested on poly(rA)/oligo(dT) under the conditions described in Materials and Methods in the presence of 0.2 μ M (3'-OH ends) of poly(rA)/oligo(dT) at different fixed concentrations of dTTP (1, 2.5, 5, and 10 μ M) and increasing amounts of the inhibitor PBO354 (0.25, 1, 5, and 15 μ M). The data were plotted according to the Lineweaver-Burk method. (B) HIV-1 RT wild type was tested on poly(rA)/oligo(dT) under the conditions described in Materials and Methods in the presence of 50 μ M dTTP with different fixed concentrations of poly(rA)/oligo(dT) (0.2, 0.08, 0.04, 0.02, and 0.008 μ M) and increasing amounts of the inhibitor PBO354 (0.25, 1, 5, and 15 μ M). The data were plotted according to the Lineweaver-Burk method. (C) HIV-1 RT wild type was tested on poly(rA)/oligo(dT) in the presence of different PBO derivatives under the conditions described in Materials and Methods in the presence of different fixed concentrations of dTTP (0.2, 1, 2, 5, and 10 μ M) and increasing concentrations of the inhibitors (0.1, 0.25, 1, 5, 25, and 75 μ M). The K_{app} values for the different inhibitors at each substrate concentration were calculated from equation 1 as described in Materials and Methods. The variation of the K_{app} values in dependence of the dTTP concentrations was analyzed according to equation 2 to calculate the true K_i values.

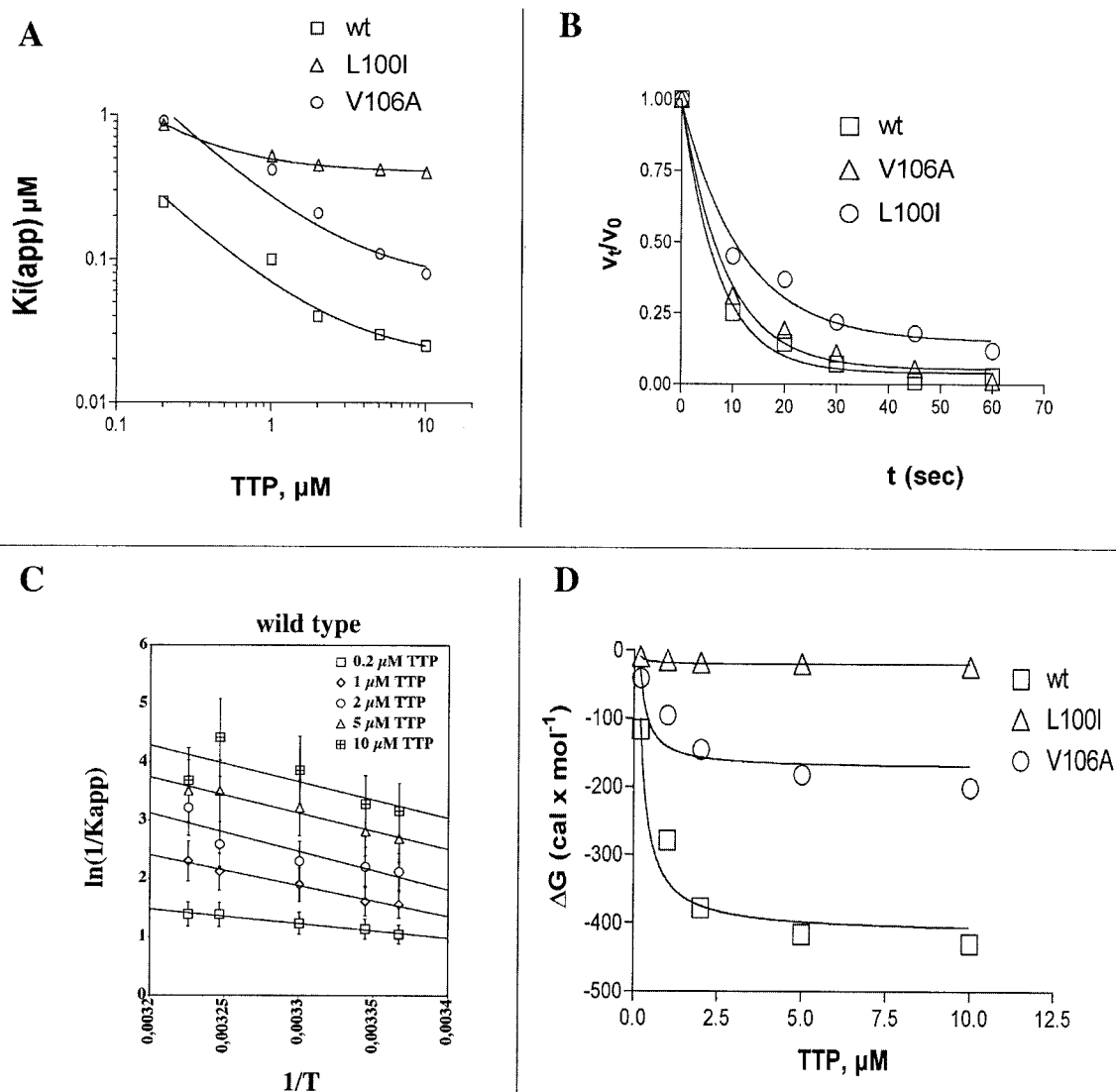


FIG. 3. All of the datum points represent the mean values of three independent experiments. Error bars indicate the standard deviations. (A) HIV-1 RT wild type and the L100I and V106A mutants were tested on poly(rA)/oligo(dT) under the conditions described in Materials and Methods, with different fixed concentrations of dTTP (0.2, 1, 2, 5, and 10 μM) and increasing concentrations of the inhibitors (0.1, 0.25, 1, 5, 25, and 75 μM). The K_{app} values for the different inhibitors at each substrate concentration were calculated from equation 1 as described in Materials and Methods. The variation of the K_{app} values was plotted in dependence of the dTTP concentrations and analyzed according to equation 2 to calculate the true K_i values. (B) Determination of the binding rate of PBO354 to HIV-1 RT wild type and mutants. Reactions were carried out as described in Materials and Methods. The data were fitted to a simple exponential equation to derive the apparent binding rate K_{app} , which was used to estimate the k_{on} and k_{off} values (see Materials and Methods). (C) HIV-1 RT wild type was tested on poly(rA)/oligo(dT) under the conditions described in Materials and Methods, with different fixed concentrations of dTTP (0.2, 1, 2, 5, and 10 μM) and increasing concentrations of the PBO354 inhibitor (0.1, 0.25, 1, 5, 25, and 75 μM). Reactions were carried out at different temperatures (24, 26, 30, 35, and 37°C). The K_{app} values for PBO354 at each substrate concentration were calculated as described in Materials and Methods and plotted with respect to different reaction temperatures. Calculation of the thermodynamic parameters was performed by using equation 4. (D) Variation of the ΔG^\ddagger for complex formation between the PBO354 inhibitor and HIV-1 RT wild type or carrying the L100I and V106A mutations. Experiments were carried out as described in panel C with RT wild type or with the L100I and V106A mutants. The corresponding ΔG^\ddagger values were determined as explained in Materials and Methods and plotted in dependence of the dTTP concentrations. The data were fitted to equation 5.

greatest potency of inhibition (Table 1), as well as the highest increase in affinity for RT, dependent on the TTP substrate (Fig. 2C). Thus, it was selected for further characterization.

HIV-1 RT drug resistance mutations V106A and L100I differentially affect enzyme sensitivity to the inhibitor PBO354. First, the apparent inhibition constants (K_{app}) of PBO354 for the L100I and V106A enzymes were determined in the pres-

ence of increasing concentration of the nucleotide substrate TTP. As shown in Fig. 3A, in the case of the mutant V106A, PBO354 showed an increase in potency of inhibition (i.e., a decrease in K_{app} values) that was comparable to the one observed with wild-type RT, even if the absolute K_{app} values were higher for V106A due to the drug resistance induced by the mutation. Interestingly, with the L100I mutant, there was no

significant variation of the K_{app} values of PBO354 depending on the TTP substrate concentrations. We have also observed this effect with the other PBO derivatives shown in Fig. 1 (data not shown), indicating that the lack of increase of the inhibition potency in dependence of the substrate concentration was not specific for the particular compound tested but rather was an intrinsic property of the L100I mutant enzyme.

Resistance to PBO354 is due to changes in the association and dissociation rates of the inhibitor for the HIV-1 RT mutants. Next, the kinetics of PBO354 binding to wild-type RT and the L100I and V106A mutants were investigated. A preformed ternary complex of RT with its substrates was challenged for increasing times with a saturating concentration of the inhibitor. The residual activity of RT was defined as the ratio of the reaction velocity at time t (v_t) after incubation with the inhibitor and the velocity in the absence of the inhibitor (v_0) and was measured as described in Materials and Methods. The variation of v_t/v_0 with time is shown in Fig. 3B. The data were fitted to a simple exponential equation to calculate the apparent rate of inhibitor association (k_{app}). This value was used to calculate the true association (k_{on}) and dissociation (k_{off}) rates, which are listed in Table 1. The inhibitor showed similar k_{on} values for the wild-type and V106A enzymes but dissociated 2.5-fold faster (higher k_{off} rate) from the latter. On the other hand, respectively, a 2.5-fold-slower association rate and a 7-fold-faster dissociation rate of the inhibitor were measured for the L100I mutant with respect to wild-type RT. These data clearly indicated a difference in the mechanism of resistance to PBO354 between the V106A and the L100I mutants.

Effects of drug resistance mutations L100I and V106A on the thermodynamics of PBO354 binding to HIV-1 RT. The effects of the reaction temperature on the binding of the PBO354 inhibitor to HIV-1 RT were investigated for the wild-type enzyme and the L100I and V106A mutants. The K_{app} values for inhibition were determined as described above (see Materials and Methods) in the presence of increasing TTP substrate concentrations and at different temperatures. Through these measurements it was possible to calculate the K_{app} values for each temperature and for each substrate concentration, which were used to estimate the ΔG^\ddagger , ΔH^\ddagger , and ΔS^\ddagger values for the inhibitor binding. As an example, the analysis performed for wild-type HIV-1 RT with PBO354 is shown in Fig. 3C. The calculated values are listed in Table 1. As can be seen, both the V106A and the L100I mutations increased the activation enthalpy (ΔH^\ddagger) for inhibitor binding. However, the more favorable entropic contribution (ΔS^\ddagger) for the V106A mutant, with respect to L100I, determined a significant difference in the ΔG^\ddagger values between the two mutants. As a result, binding of the inhibitor to the L100I enzyme was sixfold less favored than to the V106A enzyme and >20-fold less favored with respect to the wild-type enzyme. Next, we analyzed the variation of the ΔG^\ddagger values with respect to the TTP concentration. As shown in Fig. 3D, in the case of wild-type RT and of the V106A mutant, increasing the nucleotide substrate concentrations yielded more negative ΔG^\ddagger values, thus rendering the binding of the inhibitor thermodynamically favored. On the other hand, no significant variations in the ΔG^\ddagger were observed in the case of the L100I mutant. These results were in good agreement with the observed dependence of the K_{app} values

form the TTP concentration (Fig. 3A) and provide a thermodynamic explanation for the increase in inhibition potency of PBO354 in the case of the wild-type and V106A enzymes.

The mechanism of inhibition of HIV-1 RT by PBO354 is similar for both RNA-dependent and DNA-dependent DNA synthesis. HIV-1 RT can perform both RNA-dependent (RDS) and DNA-dependent (DDS) DNA synthesis. The experiments described above were performed under RDS conditions, with the homopolymeric RNA/DNA hybrid template poly(rA)/oligo(dT). However, it is known that the nature (either RNA or DNA) of the template to be copied can influence the sensitivity of RT to its inhibitors. For this reason, the variations of the K_{app} of PBO354 with respect to the TTP concentration were measured under DDS conditions with the homopolymeric DNA template poly(dA)/oligo(dT). As shown in Fig. 4A, in the case of the wild-type enzyme the inhibitor showed an increase in the affinity that was dependent on the TTP concentration, similar to what was observed under RDS conditions (Fig. 3A). In the case of the mutant V106A, the enzyme showed lower sensitivity to PBO354 on this template (i.e., higher K_{app} values) with respect to the RDS conditions (Fig. 3A). However, a similar increase in potency of inhibition for PBO354 was observed in dependence of the TTP concentration also for this mutant. Again, there was no increase in the inhibition of the mutant L100I by PBO354 with respect to the nucleotide substrate concentration. We wanted also to test whether the homopolymeric versus heteropolymeric nature of the template could affect the mechanism of inhibition of HIV-1 RT by PBO354. To do this, the RT wild type or the L100I and V106A mutants were challenged with increasing concentrations of the inhibitor on a heteropolymeric DNA template (activated DNA, which is a genomic DNA treated with DNase 1 to create gaps [see Materials and Methods]). As shown in Fig. 4C, the sensitivities of the different enzymes toward PBO354 were decreased (higher K_{app} values) with respect to the homopolymeric DNA template (see Fig. 4A); however, once again the K_{app} values for RT inhibition decreased as the dNTP concentration increased for wild-type RT and V106A enzyme but not for the mutant L100I enzyme.

The L100I mutation confers resistance to PBO354 by decreasing the catalytic efficiency of HIV-1 RT. Since the L100I mutation apparently abolished the observed dependence of the inhibition potency by PBO354 from the nucleotide substrate concentration, we wanted to investigate in more detail the enzymological properties of this enzyme. Figure 4B shows the variation of the reaction velocity for wild-type HIV-1 RT, L100I, and V106A with respect to the TTP concentration under both RDS and DDS conditions. In both cases, the L100I mutant showed a lower catalytic efficiency with respect to wild-type RT and the V106A mutant. The calculated K_m , k_{cat} , and k_{cat}/K_m values for TTP utilization are listed in Table 2. In general, the catalytic efficiency decreased from RDS to DDS for all of the enzymes, an effect that has been previously observed. However, under both RDS and DDS conditions, the k_{cat} and k_{cat}/K_m values for TTP were significantly lower for the L100I mutant than for either wild-type RT or the V106A mutant. In order to more precisely define this difference, similar substrate titration experiments were performed at different reaction temperatures, and the thermodynamic parameters for TTP utilization were determined from the variations of the k_{cat}

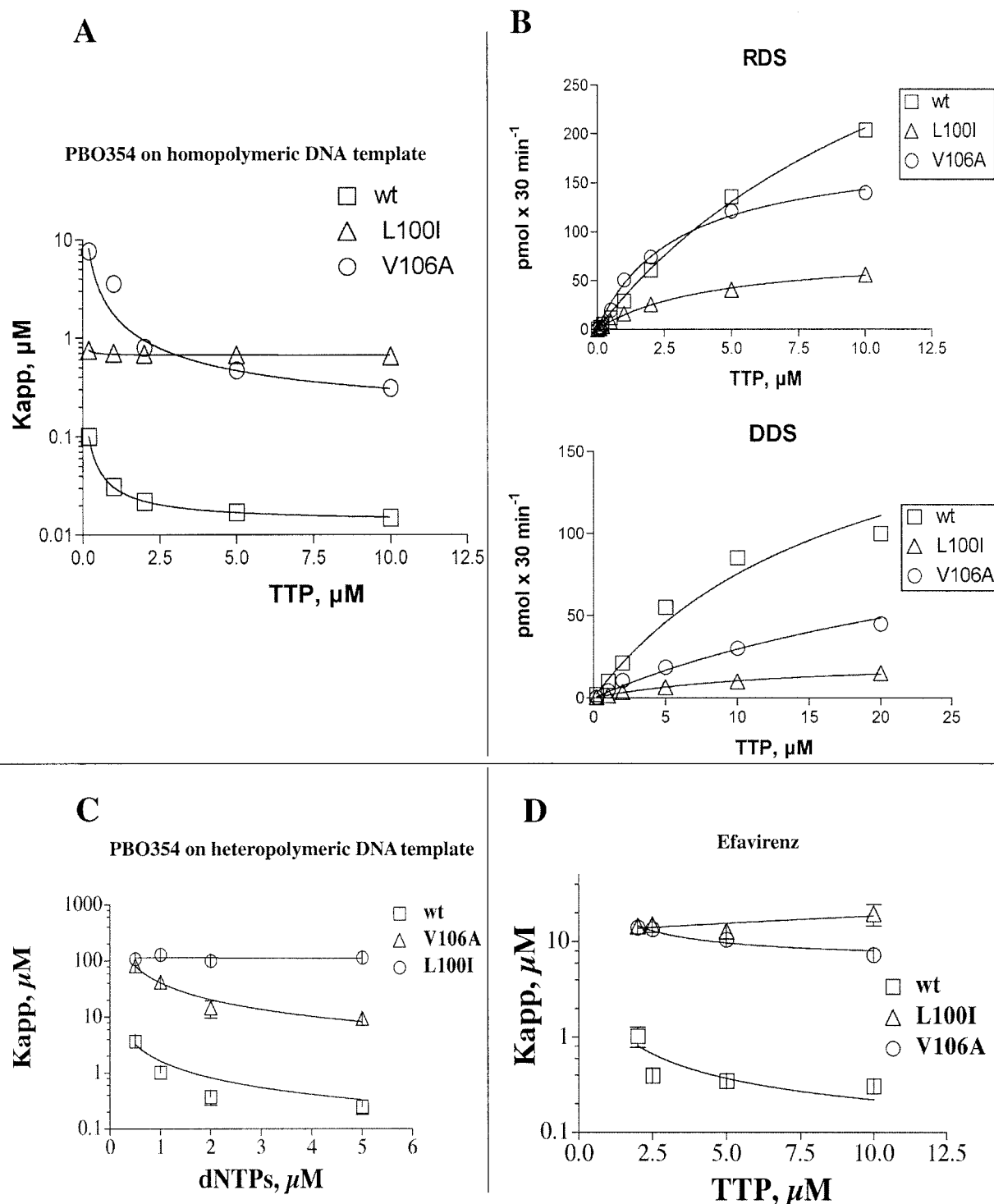


FIG. 4. All of the datum points represent the mean values of three independent experiments. Error bars are indicated as standard deviations. (A) HIV-1 RT wild type and the L100I and V106A mutants were tested on poly(dA)/oligo(dT) under the conditions described in Materials and Methods, with different fixed concentrations of dTTP (0.2, 1, 2, 5, and 10 μM) and increasing concentrations of the PBO354 inhibitor (0.1, 0.25, 1, 5, 25, and 75 μM). The K_{app} values at each substrate concentration were calculated as described in Materials and Methods. The variation of the K_{app} values was plotted in dependence of the dTTP concentrations and analyzed according to equation 2 to calculate the true K_i values. (B) HIV-1 RT wild type and the L100I and V106A mutants were assayed on poly(rA)/oligo(dT) (RDS, upper panel) or poly(dA)/oligo(dT) (DDS, lower panel) as described in Materials and Methods. The initial velocities of the reaction were derived from time course experiments (see Materials and Methods) in the presence of increasing concentrations of dTTP (0.1, 0.2, 1, 2, 5, and 10 μM for RDS and 0.2, 0.5, 1, 2, 5, 10, and 20 μM for DDS). The variation in the initial velocities of the reaction was then plotted with respect to the substrate concentrations. The data were fitted to the Michaelis-Menten equation in the form, i.e., $v = k_{\text{cat}}[E]_0/(1 + K_m/[d\text{TTP}])$, to calculate the K_m and k_{cat} parameters. (C) HIV-1 RT wild type and the L100I and V106A mutants were tested on activated DNA as described in Materials and Methods, with different fixed concentrations of the

TABLE 2. Kinetic and thermodynamic parameters for dTTP utilization by RT wild type and mutants

| Parameter | Mean value (SD) ^a | | | | | |
|---|------------------------------|---------------|---------------|--------------|---------------|----------------|
| | RDS | | | DDS | | |
| | Wild type | V106A | L100I | Wild type | V106A | L100I |
| K_m (μM) | 1 (2) | 13 (1) | 4.5 (0.5) | 18 (2) | 25 (2) | 12 (1) |
| k_{cat} (s^{-1}) | 0.48 (0.05) | 0.5 (0.06) | 0.04 (0.01) | 0.18 (0.03) | 0.2 (0.06) | 0.016 (0.002) |
| k_{cat}/K_m ($\text{s}^{-1} \mu\text{M}^{-1}$) | 0.028 (0.003) | 0.038 (0.004) | 0.009 (0.001) | 0.01 (0.001) | 0.008 (0.001) | 0.001 (0.0002) |
| ΔH^\ddagger (kcal mol^{-1}) | 11 (1) | 10 (1) | 7 (0.7) | | | |
| ΔS^\ddagger ($\text{cal mol}^{-1} \text{K}^{-1}$) | 40 (5) | 35 (3) | 23 (2) | | | |
| $\Delta G^\ddagger_{(310)}$ (kcal mol^{-1}) ^b | -1.4 (0.2) | -0.85 (0.2) | -0.13 (0.02) | | | |

^a Values for the kinetic parameters represent the mean of three independent experiments.

^b $\Delta G^\ddagger_{(310)}$, energy of activation at $T = 310 \text{ K}$.

values. The estimated ΔG^\ddagger , ΔH^\ddagger , and ΔS^\ddagger values for the reaction are listed in Table 2. HIV-1 wild-type RT and the V106A enzymes showed similar values for the ΔG^\ddagger for the reaction. Significantly, the overall reaction was less favored (compare the ΔG^\ddagger values) for L100I than for the wild-type enzyme.

The nonnucleoside inhibitor efavirenz shows a mechanism of inhibition similar to that of PBO354. Efavirenz is a expanded-spectrum NNRTI that is used in clinical practice. We have previously shown that efavirenz has a higher affinity for the ternary complex of RT and its DNA and dNTP substrates than for either the binary RT-DNA complex or the free enzyme (27). Thus, we have investigated the relationship of efavirenz inhibition to the nucleotide substrate concentration. As shown in Fig. 4D, the K_{app} for efavirenz decreased as the nucleotide concentration increased for wild-type RT and the V106A mutant. Again, no influence of the nucleotide concentration was found on the K_{app} values for inhibition of L100I by efavirenz. These data suggested that the preferential binding of efavirenz to the ternary complex proceeds through a mechanism analogous to the one observed for PBO354 and that the L100I mutation affects this mechanism in a similar way for both inhibitors.

The L100I mutation abolishes the specific targeting of the ternary complex of HIV-1 RT and its substrates by the PBO class of inhibitors. Finally, we examined the mechanism of inhibition of the mutant L100I by the PBO269 and PBO354 inhibitors. The inhibition assays were performed as described for the experiments shown in Fig. 2A and B, namely, keeping one substrate constant at saturating levels and varying the concentration of the other. In the case of wild-type RT, PBO354 acted as a noncompetitive inhibitor (Fig. 2A and B). In contrast, as shown in Fig. 5A and B, the inhibition of L100I by PBO354 was noncompetitive with respect to both substrates. Similar results were obtained with the inhibitor PBO269 (Fig. 5C and D). According to the ordered mechanism of the polymerization reaction, these data indicated that

the L100I mutation abolished the specific targeting of the ternary RT/TP/dNTP complex by the PBO derivatives, which now can bind to the enzyme independently from the substrates, thus acting as a noncompetitive inhibitor. In conclusion, these results indicated that the lack of increase of the inhibition potency and the absence of a decrease (more negative values) of the ΔG^\ddagger for inhibitor binding in dependence of the substrate concentration observed with the L100I mutant correlated with the impairment of PBO binding to the ternary complex of RT and its substrates.

DISCUSSION

Previous observations indicated that the inhibition of HIV-1 RT by the NNRTI PPO464 was due to the specific binding of this molecule to the ternary complex formed by RT, the template primer, and the dNTP (25). In the present study we extended the analysis to molecules belonging to a related class of NNRTIs, the PBO derivatives, whose structures are shown in Fig. 1. The observed increase in inhibition potencies for these compounds with respect to the nucleotide substrate concentration, at saturating concentrations of the nucleic acid substrate (Fig. 2C and Table 1) suggested a preference for the ternary complex, as with PPO464. Comparison of the structures of the unliganded enzyme with those of the enzyme-DNA and enzyme-DNA-dNTP complexes, showed differences in the relative positions of the fingers and thumb subdomains, involving the structural elements surrounding the NNRTI binding pocket (15, 16, 17, 19, 33). Thus, it is possible that local structural differences might facilitate the access of PBO inhibitors to the binding site, partially explaining the observed mechanism of inhibition. Previous observations have shown that the carboxanilide derivatives bind with different affinities to the various enzyme-substrate complexes in the RT reaction pathway (13). Moreover, in a previous study we showed that the extended-spectrum NNRTI efavirenz displayed preferential affinity for either the binary or the ternary complex of RT with

dNTPs (0.5, 1, 2, 5, and 10 μM) and increasing concentrations of the PBO354 inhibitor (0.1, 0.25, 1, 5, 25, and 75 μM). The K_{app} values at each substrate concentration were calculated as described in Materials and Methods. The variation in the K_{app} values was plotted in dependence of the dTTP concentrations and analyzed according to equation 2 to calculate the true K_i values. (D) HIV-1 RT wild type and the L100I and V106A mutants were tested on poly(rA)/oligo(dT) under the conditions described in Materials and Methods, with different fixed concentrations of dTTP (1.5, 2.5, 5, and 10 μM) and increasing concentrations of the efavirenz inhibitor (0.1, 0.25, 1, 5, 25, and 75 μM). The K_{app} values at each substrate concentration were calculated as described in Materials and Methods. The variation in the K_{app} values was plotted with respect to the dTTP concentrations and analyzed according to equation 2 to calculate the true K_i values.

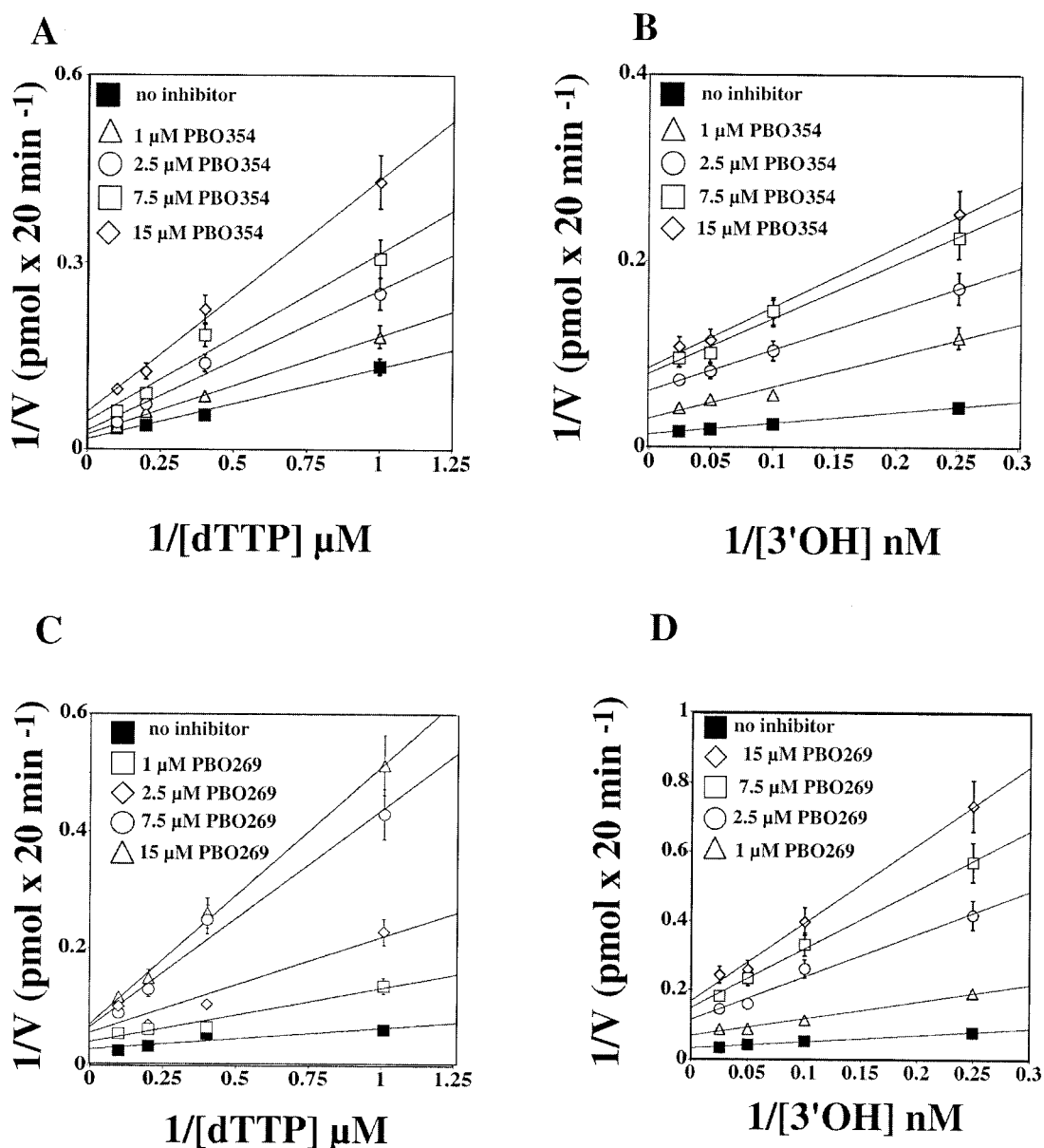


FIG. 5. All of the datum points represent the mean values of three independent experiments. Error bars are indicated as standard deviations. (A) The HIV-1 RT L100I mutant was tested on poly(rA)/oligo(dT) under the conditions described in Materials and Methods in the presence of 0.2 μM ($3'$ -OH ends) of poly(rA)/oligo(dT) at different fixed concentrations of dTTP (1, 2.5, 5, and 10 μM) and with increasing concentrations of the inhibitor PBO354 (1, 2.5, 7.5, and 15 μM). The data were plotted according to the Lineweaver-Burk method. (B) HIV-1 RT L100I was tested on poly(rA)/oligo(dT) under the conditions described in Materials and Methods in the presence of 50 μM dTTP, with different fixed concentrations of poly(rA)/oligo(dT) (0.04, 0.02, 0.01, and 0.004 μM) and increasing concentrations of the inhibitor PBO354 (1, 2.5, 7.5, and 15 μM). The data were plotted according to the Lineweaver-Burk method. (C) Same as in panel A, but with the PBO269 inhibitor. (D) Same as in panel B, but with the PBO269 inhibitor.

its substrates with respect to the unliganded enzyme (27). Thus, it is conceivable that there is an induced fit mechanism for the binding of some classes of NNRTIs that is triggered by complex formation among RT and the nucleic acid and nucleotide substrates.

The inhibitor PBO354 showed an overall decreased potency toward RT containing the drug resistance mutations L100I and V106A, even though this was to a much lower extent than narrow-spectrum NNRTIs such as nevirapine (Table 1) (see also reference 7). Interestingly, PBO354 showed an increase in

inhibition potency with respect to the nucleotide substrate concentration in the case of the V106A mutant but not with the L100I (Fig. 3A). Investigation of the binding kinetics of the inhibitors to these two mutants showed that the V106A mutation induced resistance by increasing the k_{off} rate of the inhibitor, whereas the L100I mutation affected both the k_{on} and the k_{off} rates (Fig. 3B). These data collectively suggested that the L100I mutation might alter the structure of the ternary complex of RT with its substrates, interfering with the induced fit mechanism of inhibition by the PBO analogs. This hypothesis

is further supported by the observation that the L100I enzyme showed a lower catalytic rate and nucleotide substrate utilization efficiency than RT wild type and V106A (Fig. 4B and Table 2) and that the PBO derivatives inhibited this mutant with a noncompetitive mechanism (Fig. 5A and B). Thermodynamic analysis of inhibitor binding showed that saturation of the enzyme with the nucleotide substrate favored the reaction (increase in negative ΔG^\ddagger values, Fig. 3D), only in the case of RT wild type and V106A and not for the L100I mutant. Table 1 shows that the unfavorable binding was due mainly to an increase in the enthalpy (ΔH), which is not compensated for by a correspondent variation in the entropic term. The importance in the balance between ΔH and ΔS in inhibitor binding has been also shown in the case of HIV-1 RT PIs (30). The decrease in potency of the PBO inhibitors, is therefore apparently caused by the combination of both an increase in the activation energy for complex formation (likely due to a steric barrier induced by the L100I substitution) and a lack of entropic compensation.

Specific RT mutations have variable effects on different inhibitors (5, 10, 29). The L100I single point mutation, for example, has only a moderate effect on nevirapine but causes a 100-fold loss of activity for 9-Cl TIBO, a structurally different NNRTI (4). Our results from direct binding studies (Table 1), showed that the L100I mutation reduced the rate of the association (k_{on}) of the PBO354 inhibitor to the enzyme, whereas the V106A mutation increased its dissociation rate (k_{off}). We have previously shown that in the case of nevirapine, both L100I and V106A mutations caused an increase in the k_{off} rate without significantly affecting the k_{on} value (24). Thus, the observed effect of the L100I mutation on PBO354 binding seems to be specific for this class of compounds. Docking models of PBO compounds into the RT NNRTI-binding site, based on the structure of the RT-nevirapine complex, showed that no hydrogen bonds involved the oxygens of the inhibitor but that both the fused pyrrole and the pendant phenyl ring at C-6 of the PBO structure were in close contact with the side chains of Y181, V106, K103, K101, and L100 (7). L100I is an isosteric replacement, with the isoleucine γ -methyl group pointing directly toward a ring of each ligand and adjacent to any group that is hydrogen bonded with K101. Thus, the L100I mutation is likely to cause either a steric penalty and/or to destabilize the hydrogen bonding to K101. In contrast, the V106A mutations represent significant size reductions, which diminish favorable hydrophobic contacts between the enzyme and the inhibitors. Thus, it is conceivable to hypothesize that the L100I substitution would act mainly by introducing a steric barrier to PBO binding. This mechanism has been previously proposed for structurally different NNRTIs based on molecular modeling simulations (36).

The observation that the L100I enzyme showed a lower catalytic efficiency (Table 2) suggested a correlation between the observed resistance of L100I to the PBO354 inhibitor and the loss of catalytic efficiency for TTP utilization of the mutated enzyme. It should be noted here that the exact nature of the rate-limiting step (k_{cat}) is not known, nor can it be determined under these experimental conditions. Thus, the observed differences in ΔG^\ddagger values could also be due, in principle, to a change in the nature of the rate-limiting step of the reaction. However, regardless of the identity of the slowest

step of the reaction, the analysis shown here clearly indicated a difference in the thermodynamics of the nucleotide incorporation reaction among the different enzymes tested.

Given the particular nature of the mechanism of RT inhibition by the PBO class of NNRTIs, it might be hypothesized that the L100I mutation specifically altered the geometry of the active site of the enzyme. The RT enzyme undergoes to substantial structural rearrangements upon binding to its substrates, nucleic acid and nucleotide. Gaussian network modeling of the collective motions of HIV-1 RT identified some regions of the protein that appeared to act as molecular hinges for the large-scale movements of the RT subdomains (3, 34). One of these regions corresponded to the loop in the p66 palm subdomain which contains the L100 residue. Thus, the L100I substitution might interfere with this hinge function, perhaps causing a sort of "molecular arthritis" to HIV-1 RT, impairing the correct positioning of the catalytic triad formed by the residues D110, D185, and D186 and reducing nucleotide incorporation.

In summary, our data provide further insights into the mechanism of inhibition of HIV-1 RT by the PBO class of compounds, suggesting the possibility of designing novel molecules with low toxicity and high potency to be used in combination therapies as an alternative to the currently used efavirenz and nevirapine. One observation stemming from the present study is that PBO resistance induced by the L100I mutation was achieved through a significant loss of catalytic efficiency of the mutated enzyme. This implies that such a mutation will be fixed in the viral population only in the presence of a strong selective pressure. Indeed, viruses carrying the L100I mutation in the RT gene are very frequently isolated in HIV-1-infected patients treated with NNRTIs but are very rare in naive patients (2, 31). The V106A mutation is also very rare, and it has been shown that the virus carrying this mutation displays a significantly reduced fitness. This is apparently in contradiction to our findings that the catalytic properties of the V106A RT are similar to the wild-type enzyme (Table 2). However, it has been recently shown that the replicative defect of the V106A mutant viruses is likely due to an impairment of the RNase H activity of the viral RT (1), thus explaining this apparent paradox.

ACKNOWLEDGMENTS

We thank S. H. Hughes (NCI-Frederick Cancer Research and Development Center) for kindly providing the coexpression vectors pUC12N/p66(His)/p51 with the wild-type or the mutant forms of HIV-1 RT p66.

This study was partially supported by the ISS-Programma Nazionale di Ricerca sull'AIDS grant 30D.72 (to S.S.) and by EU TRIOH 503480 grant (to G.M.). G.A.L. was a "Buzzati-Traverso" fellow.

REFERENCES

1. Archer, R. H., C. Dykes, P. Gerondelis, A. Lloyd, P. Fay, R. C. Reichman, R. A. Bambara, and L. M. Demeter. 2000. Mutants of human immunodeficiency virus type 1 (HIV-1) reverse transcriptase resistant to nonnucleoside reverse transcriptase inhibitors demonstrate altered rates of RNase H cleavage that correlate with HIV-1 replication fitness in cell culture. *J. Virol.* 74:8390-8401.
2. Bachelier, L. T., E. D. Anton, P. Kudish, D. Baker, J. Bunville, K. Krakowski, L. Bolling, M. Aujay, X. V. Wang, D. Ellis, M. F. Becker, A. L. Lasut, H. J. George, D. R. Spalding, G. Hollis, and K. Abremski. 2000. Human immunodeficiency virus type 1 mutations selected in patients failing efavirenz combination therapy. *Antimicrob. Agents Chemother.* 44:2475-2484.
3. Bahar, I., B. Erman, R. L. Jernigan, A. R. Atilgan, and D. G. Covell. 1999.

- Collective motions in HIV-1 reverse transcriptase: examination of flexibility and enzyme function. *J. Mol. Biol.* **285**:1023–1037.
4. **Balzarini, J., A. Karlsson, C. Meichsner, A. Paessens, G. Riess, E. De Clercq, and J. P. Kleim.** 1994. Resistance pattern of human immunodeficiency virus type 1 reverse transcriptase to quinoxaline S-2720. *J. Virol.* **68**:7986–7992.
 5. **Boyer, P. L., J. Ding, E. Arnold, and S. H. Hughes.** 1994. Drug resistance of human immunodeficiency virus type 1 reverse transcriptase: subunit specificity of mutations that confer resistance to nonnucleoside inhibitors in human immunodeficiency virus type 1 reverse transcriptase. *Antimicrob. Agents Chemother.* **38**:1909–1914.
 6. **Boyer, P. L., A. L. Ferris, P. Clark, J. Whitmer, P. Frank, C. Tantillo, E. Arnold, and S. H. Hughes.** 1994. Mutational analysis of the fingers and palm subdomains of human immunodeficiency virus type-1 (HIV-1) reverse transcriptase. *J. Mol. Biol.* **243**:472–483.
 7. **Campiani, G., E. Morelli, M. Fabbrini, V. Nacci, G. Greco, E. Novellino, A. Ramunno, G. Maga, S. Spadari, G. Caliendo, A. Bergamini, E. Faggioli, I. Uccella, F. Bolacchi, S. Marini, M. Coletta, A. Nacca, and S. Caccia.** 1999. Pyrrolobenzoxazepinone derivatives as non-nucleoside HIV-1 RT inhibitors: further structure-activity relationship studies and identification of more potent broad-spectrum HIV-1 RT inhibitors with antiviral activity. *J. Med. Chem.* **42**:4462–4470.
 8. **Campiani, G., A. Ramunno, G. Maga, V. Nacci, C. Fattorusso, B. Catalanotti, E. Morelli, and E. Novellino.** 2002. Non-nucleoside HIV-1 reverse transcriptase (RT) inhibitors: past, present, and future perspectives. *Curr. Pharm. Des.* **8**:615–657.
 9. **Crowe, S.** 1999. New reverse transcriptase inhibitors. *Adv. Exp. Med. Biol.* **458**:183–197.
 10. **De Clercq, E.** 1994. New developments in the chemotherapy of lentivirus (human immunodeficiency virus) infections: sensitivity/resistance of HIV-1 to non-nucleoside HIV-1-specific inhibitors. *Ann. N. Y. Acad. Sci.* **724**:438–456.
 11. **DeClercq, E.** 1993. HIV-1-specific reverse transcriptase inhibitors: highly selective inhibitors of human immunodeficiency virus type 1 that are specifically targeted at the viral reverse transcriptase. *Medicinal Res. Rev.* **13**:229–258.
 12. **Esnouf, R., J. Ren, C. Ross, Y. Jones, D. Stammers, and D. Stuart.** 1995. Mechanism of inhibition of HIV-1 reverse transcriptase by non-nucleoside inhibitors. *Nat. Struct. Biol.* **2**:303–308.
 13. **Fletcher, R. S., K. Syed, S. Mithani, G. I. Dmitrienko, and M. A. Parniak.** 1995. Carboxanilide derivative non-nucleoside inhibitors of HIV-1 reverse transcriptase interact with different mechanistic forms of the enzyme. *Biochemistry* **34**:4346–4353.
 14. **Harrington, M., and C. C. Carpenter.** 2000. Hit HIV-1 hard, but only when necessary. *Lancet* **355**:2147–2152.
 15. **Hsiou, Y., J. Ding, K. Das, A. D. Clark, Jr., S. H. Hughes, and E. Arnold.** 1996. Structure of unliganded HIV-1 reverse transcriptase at 2.7 Å resolution: implications of conformational changes for polymerization and inhibition mechanisms. *Structure* **4**:853–860.
 16. **Huang, H., R. Chopra, G. L. Verdine, and S. C. Harrison.** 1998. Structure of a covalently trapped catalytic complex of HIV-1 reverse transcriptase: implications for drug resistance. *Science* **282**:1669–1675.
 17. **Huang, H., S. C. Harrison, and G. L. Verdine.** 2000. Trapping of a catalytic HIV reverse transcriptase template-primer complex through a disulfide bond. *Chem. Biol.* **7**:355–364.
 18. **Hübscher, U., and S. Spadari.** 1994. DNA replication and chemotherapy. *Physiol. Rev.* **74**:259–304.
 19. **Jacobo-Molina, A., J. Ding, R. G. Nanni, A. D. Clark, Jr., X. Lu, C. Tantillo, R. L. Williams, G. Kamer, A. L. Ferris, P. Clark, et al.** 1993. Crystal structure of human immunodeficiency virus type 1 reverse transcriptase complexed with double-stranded DNA at 3.0 Å resolution shows bent DNA. *Proc. Natl. Acad. Sci. USA* **90**:6320–6324.
 20. **Jonckheere, H., J. Anne, and E. De Clercq.** 2000. The HIV-1 reverse transcription (RT) process as target for RT inhibitors. *Med. Res. Rev.* **20**:129–154.
 21. **Kati, W. M., K. A. Johnson, L. F. Jerva, and K. S. Anderson.** 1992. Mechanism and fidelity of HIV reverse transcriptase. *J. Biol. Chem.* **267**:25988–25997.
 22. **Kaufmann, G. R., and D. A. Cooper.** 2000. Antiretroviral therapy of HIV-1 infection: established treatment strategies and new therapeutic options. *Curr. Opin. Microbiol.* **3**:508–514.
 23. **Kohlstaedt, L. A., J. Wang, J. M. Friedman, P. A. Rice, and T. A. Steitz.** 1992. Crystal structure at 3.5 Å resolution of HIV-1 reverse transcriptase complexed with an inhibitor. *Science* **256**:1783–1790.
 24. **Maga, G., N. M. Amacker, Ruel, U. Hübscher, and S. Spadari.** 1997. Resistance to nevirapine of HIV-1 reverse transcriptase mutants: loss of stabilizing interactions and thermodynamic or steric barriers are induced by different single amino acid substitutions. *J. Mol. Biol.* **274**:738–747.
 25. **Maga, G., A. Ramunno, V. Nacci, G. A. Locatelli, S. Spadari, I. Fiorini, F. Baldanti, S. Paolucci, M. Zavattoni, A. Bergamini, B. Galletti, S. Muck, U. Hübscher, G. Giorgi, G. Guiso, S. Caccia, and G. Campiani.** 2001. The stereoselective targeting of a specific enzyme-substrate complex is the molecular mechanism for the synergic inhibition of HIV-1 reverse transcriptase by (R)-(–)-PPO464: a novel generation of nonnucleoside inhibitors. *J. Biol. Chem.* **276**:44653–44662.
 26. **Maga, G., and S. Spadari.** 2002. Combinations against combinations: associations of anti-HIV 1 reverse transcriptase drugs challenged by constellations of drug resistance mutations. *Curr. Drug Metab.* **3**:73–95.
 27. **Maga, G., D. Ubiali, R. Salvetti, M. Pregolato, and S. Spadari.** 2000. Selective interaction of the human immunodeficiency virus type 1 reverse transcriptase nonnucleoside inhibitor efavirenz and its thio-substituted analog with different enzyme-substrate complexes. *Antimicrob. Agents Chemother.* **44**:1186–1194.
 28. **Moyle, G.** 2001. The emerging roles of non-nucleoside reverse transcriptase inhibitors in antiretroviral therapy. *Drugs* **61**:19–26.
 29. **O'Brien, W. A.** 2000. Resistance against reverse transcriptase inhibitors. *Clin. Infect. Dis.* **30**(Suppl. 2):S185–S192.
 30. **Ohtaka, H., A. Velazquez-Campoy, D. Xie, and E. Freire.** 2002. Overcoming drug resistance in HIV-1 chemotherapy: the binding thermodynamics of amprenavir and TMC-126 to wild-type and drug-resistant mutants of the HIV-1 protease. *Protein Sci.* **11**:1908–1916.
 31. **Rayner, M. M., B. Cordova, and D. A. Jackson.** 1997. Population dynamics studies of wild-type and drug-resistant mutant HIV in mixed infections. *Virology* **236**:85–94.
 32. **Ren, J., R. Esnouf, E. Garman, D. Somers, C. Ross, I. Kirby, J. Keeling, G. Darby, Y. Jones, D. Stuart, and D. Stammers.** 1995. High resolution structures of HIV-1 RT from four RT-inhibitor complexes. *Nat. Struct. Biol.* **2**:293–302.
 33. **Rodgers, D. W., S. J. Gamblin, B. A. Harris, S. Ray, J. S. Culp, B. Hellmig, D. J. Woolf, C. Debouck, and S. C. Harrison.** 1995. The structure of unliganded reverse transcriptase from the human immunodeficiency virus type 1. *Proc. Natl. Acad. Sci. USA* **92**:1222–1226.
 34. **Temiz, N. A., and I. Bahar.** 2002. Inhibitor binding alters the directions of domain motions in HIV-1 reverse transcriptase. *Proteins* **49**:61–70.
 35. **Vella, S., and L. Palmisano.** 2000. Antiretroviral therapy: state of the HAART. *Antivir. Res.* **45**:1–7.
 36. **Wang, D. P., R. C. Rizzo, J. Tirado-Rives, and W. L. Jorgensen.** 2001. Antiviral drug design: computational analyses of the effects of the L1001 mutation for HIV-RT on the binding of NNRTIs. *Bioorg. Med. Chem. Lett.* **11**:2799–2802.
 37. **Weiser, T., M. Gassmann, P. Thommes, E. Ferrari, P. Hafkemeyer, and U. Hübscher.** 1991. Biochemical and functional comparison of DNA polymerases alpha, delta, and epsilon from calf thymus. *J. Biol. Chem.* **266**:10420–10428.